

Inhibition of indoleamine 2,3-dioxygenase 1 synergizes with oxaliplatin for efficient colorectal cancer therapy

Xiaofei Miao,^{1,2} Ye Zhang,² Zengyao Li,² Longchang Huang,¹ Taojian Xin,¹ Renhui Shen,¹ and Tong Wang^{1,2}

¹Nanjing Medical University, Nanjing, 210000 Jiangsu, China; ²Wuxi People's Hospital, Wuxi, 214023 Jiangsu, China

We investigated the immunogenic cell death provoked by oxaliplatin (OXA) and the involvement of OXA-induced immunosuppression in colorectal cancer. Immune-proficient or -deficient mice were employed to evaluate the therapeutic effects of OXA. Immunogenic cell death was characterized by cell-surface calreticulin, cytosol-translocated high migration rate group protein B1 (HMGB1), and secretory ATP content. Bone marrow-derived dendritic cell (BMDC) maturation and CD8⁺ T cell expansion were measured by flow cytometry. Expression of immunosuppressive genes was quantified by both RT-PCR and western blots. The proliferative and apoptotic indexes of xenograft tumors were evaluated by immunohistochemistry and TUNEL assays, respectively. The secretory cytokines were measured with ELISA. OXA induced immunogenic cell death of murine colorectal cancer, which greatly depended on the host immune response. OXA-pretreated CT26 cells promoted BMDC maturation and CD8⁺ T cell expansion. OXA significantly upregulated indoleamine 2,3-dioxygenase 1 (IDO1) in patient-derived colorectal cancer cells and in combination with the IDO1-specific inhibitor, NLG919, suppressed tumor progression. Simultaneous administration with both OXA and NLG919 greatly promoted CD8⁺ T cell infiltration and decreased immunosuppressive cytokine transforming growth factor β (TGF- β) production, whereas increased immunostimulatory cytokines interleukin (IL)-12p70 and interferon (IFN)- γ . We demonstrated the upregulation of IDO1 by OXA, which combined with the IDO1 inhibitor, tremendously potentiated therapeutic effects of OXA against colorectal cancer.

INTRODUCTION

Colorectal cancer (CRC) is one of the most common cancers that originates from the digestive tract.¹ Based on recent statistics, the morbidity and mortality of CRC rank as the top four of all human malignancies.² The acknowledged risk factors associated with CRC include old age and lifestyle factors, such as diet, smoking, and lack of physical exercise.³ Inflammatory bowel disease is commonly relevant to incidence of CRC as well. In addition, some inherited genetic disorders can cause CRC, accounting for less than 5% of all cases. The current mainstay therapeutics of CRC include surgery, chemotherapy, and radiotherapy.⁴ Approximately 75% of CRC patients

were diagnosed at an early stage (I–III), which is applicable for radical resection and/or chemotherapy. Some cases at an advanced stage are usually not curable and are frequently managed with the aim to improve life quality and symptoms. Chemotherapy is still the primary option for these patients.

In the last decade, cancer immunotherapy has developed rapidly,⁵ but the response rate of PD-1/PD-L1 monoclonal antibody and other immune checkpoint inhibitory antibodies in CRC patients is generally low.⁶ It is urgent to develop new strategies to activate the anti-tumor immune response in CRC patients.⁷

Oxaliplatin (OXA) and fluorouracil-base adjuvant chemotherapy are the standard treatments for postoperative stage III CRC patients and patients with selective high-risk stage II disease.⁸ Recent studies have shown that OXA not only induces tumor cell apoptosis but can also cause immunogenic death.⁹ Three types of signals are released when tumor cells undergo immunogenic death: (1) calreticulin (CRT) is exposed on the cell surface and stimulates dendritic cells (DCs) to engulf tumor cells; (2) adenosine triphosphate is released and recruits DCs to enter the tumor loci; and (3) high migration rate group protein B1 (HMGB1) promotes complexation between DCs and dying tumor cells and induces specific T cell anti-tumor immunity.¹⁰ Although OXA and other chemotherapy drugs that are able to provoke immunogenic cell death can activate the anti-tumor immune response to a certain extent, the therapeutic effects of these drugs are not satisfactory in clinical practice, possibly due to the existence of multiple complex immunosuppressive signaling pathways in the tumor microenvironment. Emerging studies have shown that combining immunogenic chemotherapy drugs with antibodies or chemicals that reverse the tumor-immunosuppressive microenvironment is expected to achieve better therapeutic efficacy.^{11,12}

Here, we first validated the immunogenic cell death provoked by OXA in CRC and further uncovered the universal upregulation of

Received 21 July 2020; accepted 31 December 2020;
<https://doi.org/10.1016/j.omtm.2020.12.013>.

Correspondence: Tong Wang, Department of General Surgery, Wuxi People's Hospital, No. 299 Qingyang Road, Wuxi, 214023 Jiangsu, China.
E-mail: twang1234@163.com



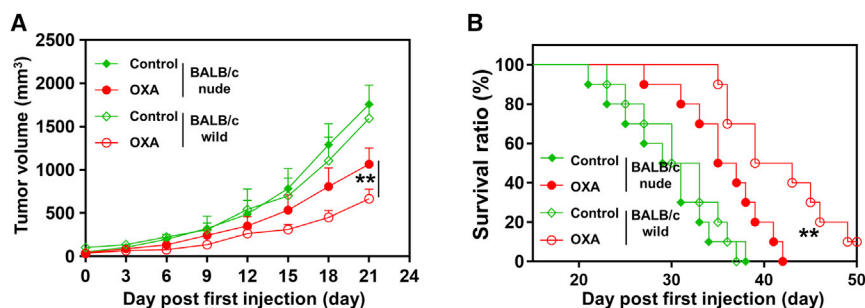


Figure 1. Oxaliplatin (OXA) exhibits improved antitumor efficacy against murine colorectal cancer in BALB/c mice

Murine colorectal tumor models were established in immunodeficient BALB/c nude mice and wild BALB/c mice, and when tumor volumes reach about 50 mm³, mice were treated with PBS or OXA (3 mg/kg) every 3 days for 4 times. The tumor growth and survival of tumor-bearing mice were monitored. (A) Tumor growth curves. (B) Survival ratio of tumor-bearing mice. Data represent mean \pm SD. ***p* < 0.01 versus OXA-treated nude mice.

immunosuppressive genes by OXA treatment through yet-unrecognized mechanisms. Notably, we identified that indoleamine 2,3-dioxygenase 1 (IDO1) was specifically induced by OXA, and therefore, combined treatment of OXA with IDO1-specific inhibitor NLG919 was shown to potentially inhibit tumor progression, which was accompanied with enhanced CD8⁺ T cell infiltration, decreased transforming growth factor β (TGF- β) production, and increased interleukin (IL)-12p70 and interferon (IFN)- γ secretion. Our study highlighted the promising therapeutic value of combinational administration of OXA and NLG919 against CRC and warranted further basic and clinical investigations.

RESULTS

OXA exhibits improved anti-tumor efficacy against murine CRC in BALB/c mice

We first compared the anti-tumor activity of OXA in immunodeficient and immune intact BALB/c mice. To this purpose, the murine CRC model was established with subcutaneous inoculation of CT26 cells. OXA was administered every 3 days for a consecutive four times after xenograft tumor volume reached 50 mm³, and both tumor growth and overall mouse survival were monitored regularly. As shown in Figure 1A, treatment with OXA significantly delayed xenograft tumor progression in wild-type BALB/c mice in comparison with vehicle, whereas a smaller difference was observed in immunodeficient groups, which implicated an essential role of host immune response in the anti-tumoral activity of OXA against CRC. Accordingly, OXA greatly prolonged the overall survival of tumor-bearing wild-type BALB/c mice, whereas the extent of improvement in survival was less obvious in the OXA-treated immune-deficient mice (Figure 1B). Therefore, our data demonstrated the improved therapeutic efficacy of OXA against murine CRC in BALB/c mice, which heavily depended on the intact immune system.

OXA induces immunogenic cell death of murine CRC cell line CT26

Our previous data suggested the evident dependence of an OXA-elicited anti-tumor effect against the colorectal xenograft tumor on the host immune system, which indicated the potential involvement of immunogenic cell death in this scenario. To clarify this speculation, we then analyzed the characteristic events of immunogenic cell death in CT26 cells upon OXA treatment. As shown in Figure 2A, flow cytometry results suggested remarkably increased cell surface CRT in

OXA-treated CT26 cells in comparison with vehicle control, and the statistical data were presented in Figure 2B. We also examined the cell surface CRT abundance with direct fluorescence antibody staining and obtained a consistent result with respect to increased CRT in OXA-treated cells compared to the vehicle control (Figure 2C). In addition, both cytosolic and secreted HMGB1 were induced by OXA treatment, as indicated in cell immunofluorescence and western blot, respectively (Figures 2D and 2E). We further determined the released ATP contents in the cell culture supernatant in response to OXA treatment using a chemiluminescent method. In support of the immunogenic cell death stimulated by OXA, we noticed a tremendous increase of secreted ATP in CT26 culture media after treatment with OXA in comparison with the vehicle control (Figure 2F). Through profiling the molecular markers, our results unambiguously demonstrated that OXA triggered immunogenic cell death in CRC cells.

OXA-treated CT26 cells promote bone marrow-derived DC (BMDC) maturation and CD8⁺ T cell proliferation

Next, we sought to evaluate the impact of OXA-treated CT26 cells on both BMDC maturation and CD8⁺ cytotoxic T cell proliferation.

To this end, we isolated BMDCs from OT-I mice and co-cultured them with OXA-pretreated CT26-OVA at a ratio of 1:1 for 3 days (Figure 3A). The maturation of BMDCs was monitored by flow cytometry with CD80⁺/CD86⁺ cells denoted as the mature population. As suggested by Figure 3B, OXA pretreatment of CT26-OVA stimulated a significant increase of BMDC maturation in comparison with control, and statistical results were provided in Figure 3C. We further isolated the matured BMDCs and co-incubated them with CD8⁺ T cells derived from OT-I mouse spleen (Figure 3D). The proliferative index of CD8⁺ T cells was determined with the carboxyfluorescein succinimidyl ester (CFSE) staining method. OXA treatment greatly promoted T cell proliferation compared to vehicle (54.6% versus 17.6%; Figures 3E and 3F). Therefore, our data provided evidence suggesting that OXA pretreatment greatly stimulated both BMDC maturation and T cell proliferation in the co-culture system.

OXA treatment upregulated IDO1 in patient-derived CRC cells

Despite the potent activation of a host immune response, the unsatisfactory anti-tumor effects of OXA prompted us to hypothesize another concomitant activation of immunosuppressive signals. To clarify this

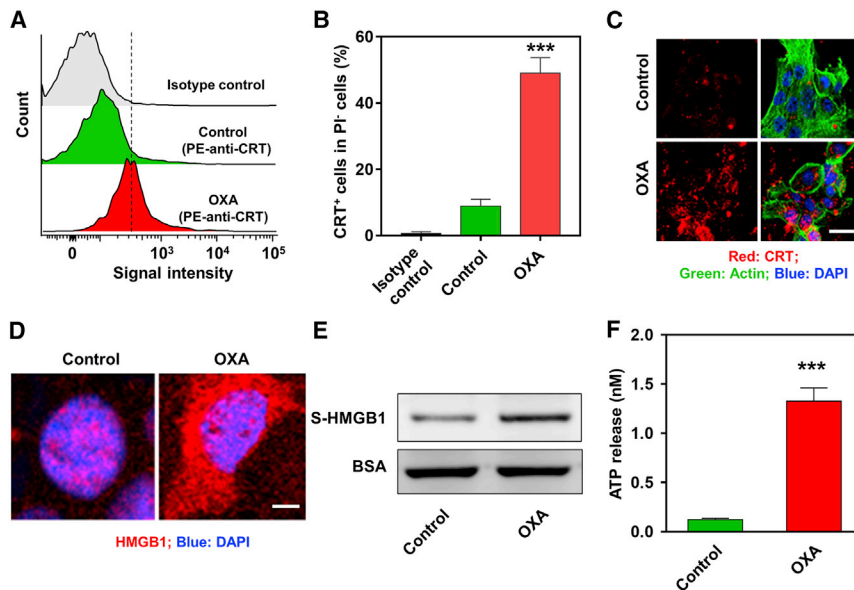


Figure 2. OXA induces immunogenic cell death of murine colorectal cancer CT26

(A) The surface exposure of calreticulin (CRT) was determined by flow cytometry among viable (propidium iodide [PI]-negative) cells after treatment with OXA (50 μ M) for 24 h. OXA-treated cells were stained with PI and phycoerythrin (PE)-labeled anti-CRT antibodies, according to the manufacturer's instructions. (B) The percentage of CRT-positive cells in PI-negative cells was quantified based on the results of flow cytometry detection. Data represent mean \pm SD. *** p < 0.001 (versus control group). (C) Confocal microscopy showing the induction of CRT in CT26 cells after 24 h OXA treatment. (D) HMGB1 release from cell nucleus to cytoplasm of CT26 tumor cells measured after immunofluorescence staining. (E) Released HMGB1 in the supernatant (S-HMGB1) of CT26 cells was measured by western blot, and BSA was used as the loading control. (F) Amount of released ATP was determined by a chemiluminescent ATP Determination Kit. Data represent mean \pm SD. *** p < 0.001 (versus control group).

issue, we collected 10 colorectal tumor tissues clinically and digested them into single cells for consecutive *in vitro* culture, which was subsequently subjected to OXA treatment for 2 days. The immunosuppression-relevant genes in response to OXA treatment were analyzed at the transcript level by real-time PCR. As shown in Figure 4A, we observed universal upregulation of all examined molecular markers, including PD-1, PD-L1, CTLA-4, CSF-1R, STAT3, CD73, and CD39, with IDO1 being the most significantly upregulated gene. The upregulation of IDO1 was further validated at the protein level by western blot in 3 patient-derived CRC cells (Figure 4B). Consistent with this, IDO1 was tremendously induced by OXA in CT26 cells, as quantified by both real-time PCR and western blot (Figure 4C). Therefore, our data uncovered that OXA upregulated IDO1 in CRC, which might directly contribute to the immunosuppressive microenvironment and compromised therapeutic effect of OXA.

***In vivo* anti-tumor effect of OXA and NLG919**

Given the aberrant overexpression of IDO1 in OXA-treated CRC cells, next, we sought to investigate the therapeutic actions of combined treatment with both OXA and the IDO1-specific inhibitor. Here, we employed NLG919 to treat CT26 xenograft tumor mice either alone or in combination with OXA. Both OXA and NLG919 were capable of inhibiting CT26 xenograft tumor growth, whereas the most significant suppression was observed in response to combined treatment of OXA and NLG919 (Figure 5A). Consistently, combinational administration of OXA and NLG919 tremendously decreased tumor weight in comparison with treatment of either OXA or NLG919 alone (Figure 5B). We further evaluated both cell proliferation and apoptosis in response to the treatments with immunohistochemistry (IHC) and terminal deoxynucleotidyl transferase (TdT)-mediated deoxyuridine triphosphate (dUTP) (TUNEL) staining, respectively. As shown in Figure 5C, an evident proliferating cell nuclear antigen (PCNA)-positive signal was noticed in the vehicle-

treated xenograft tumor, which was partially compromised by either OXA or NLG919 treatment, whereas greatly inhibited in response to their combined treatment. In contrast, the TUNEL signal was slightly induced by both OXA and NLG919, whereas tremendously increased by combinational treatment with both either or NLG919. Importantly, we also assessed the anti-tumor effect of the combined treatment in BALB/c nude mice (Figure 6). As expected, NLG919 did not improve the therapeutic effect of OXA in this model, confirming that the effect of the IDO inhibitor was mediated via the active immune system of the mice. Taken together, our results uncovered the synergistic effects of NLG919 with OXA against CRC *in vivo*.

Flow cytometry analysis of CD8⁺ T cell subsets and ELISA analysis of cytokine expression in tumor tissues

Our previous results disclosed evident anti-tumor activity of OXA combined with NLG919. Next, we sought to investigate the immune response following this treatment in tumor tissues. Our results suggested the evident increase of the CD8⁺ T cell population in CD45⁺ tumor-infiltrating lymphocytes upon either OXA or NLG919 treatment alone, whereas the combination of these two drugs greatly stimulated cytotoxic T cell expansion (Figures 7A and 7B). We further determined the cytokine production in the xenograft tumor derived from mice subjected to OXA, NLG919 treatment alone, or in combination. The immunosuppressive TGF- β was remarkably decreased upon either OXA or NLG919 treatment, which was further inhibited by their combination (Figure 7C). On the contrary, immunostimulatory cytokines, such as IL-12p70 (Figure 7D) and IFN- γ (Figure 7E), were induced by either OXA or NLG919 treatment, whereas a combination of OXA and NLG919 treatment tremendously increased their productions in xenograft tumor models. Therefore, our data suggested that a combination of OXA and NLG919 potentially stimulated CD8⁺ T cell expansion and significantly inhibited immunosuppressive cytokine and induced

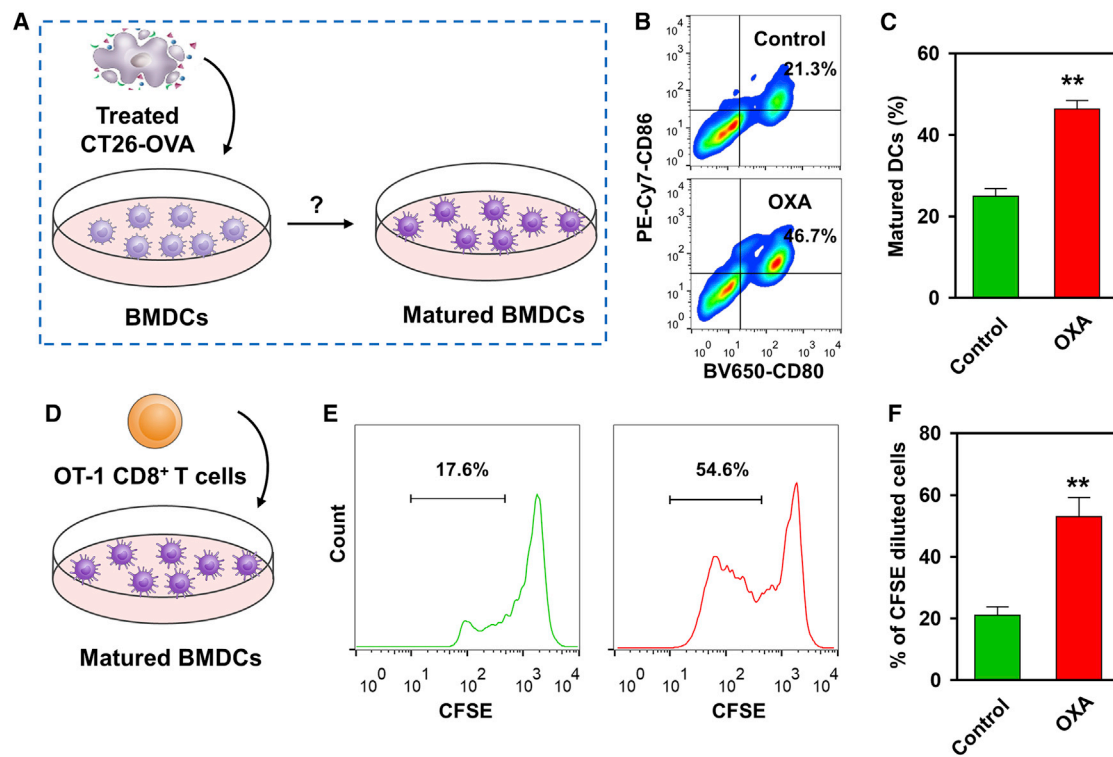


Figure 3. OXA-treated CT26 cells promote bone marrow-derived dendritic cell (BMDc) maturation and CD8⁺ T cell proliferation

(A) BMDcs were isolated from OT-I mice and cultured with the presence of OXA-treated CT26-OVA. After 3 days of culture, the maturation of DCs was examined by flow cytometry. (B and C) Flow cytometry gating (B) and histogram analysis (C) of matured BMDcs after co-incubation. The matured BMDcs were denoted as CD80⁺CD86⁺ populations. Data represent mean \pm SD. ** $p < 0.01$ versus control group. (D) Treated BMDcs were cocultured with spleen-isolated CD8⁺ T cells (from OT-I mice), and then the proliferation of T cells was examined. (E and F) Flow cytometry gating (E) and histogram analysis (F) of T cell proliferation. CD8⁺ T cells were labeled with CFSE. Data represent mean \pm SD. ** $p < 0.01$ versus control group.

immunostimulatory cytokine production, which convergently contributed to the synergistic effects against CRC between OXA and NLG919.

DISCUSSION

OXA-based adjuvant chemotherapy was the standard cure for post-surgical cancer patients at stage III and stage II at high risk. Recent investigations continuously suggested that OXA not only induced cell apoptosis but also provoked immunogenic cell death.^{9,13,14} Here, we employed a xenograft tumor mouse model and confirmed the improved anti-tumor efficacy of OXA against murine CRC in immune-intact hosts rather than immunodeficient ones, which implicated that the OXA anti-tumor actions were partially dependent on host immune response. We then systematically profiled immunogenic cell death-relevant biomarkers in CT26 cells exposed to OXA and observed significantly increased CRT, HMGB1, and secretory ATP in response to OXA. OXA-pretreated cancer cells greatly promoted BMDc maturation and cytotoxic CD8⁺ T cell expansion. Our data clearly showed that OXA potently activated an immune response, whereas unsatisfactory tumor-suppressive effects were observed with OXA administration, which indicated potential activation of immunosuppression by OXA concomitantly. Therefore, we examined multiple immunosuppressive genes and unexpectedly,

found that most of them were upregulated in response to OXA treatment. IDO1 was the most significantly stimulated gene by OXA, which was confirmed at the protein level as well. Combinational treatment of OXA with the IDO1-specific inhibitor NLG919 greatly inhibited xenograft tumor progression and significantly prolonged survival of tumor-bearing mice, which was accompanied by decreased cell proliferation and increased cell apoptosis. Tumor-infiltrating CD8⁺ T cells were tremendously expanded by combinational administration of OXA and NLG919. The local immunosuppressive TGF- β was greatly inhibited, whereas immunostimulatory IL-12p70 and IFN- γ were induced simultaneously. Therefore, our data validated the previous observation of immunogenic cell death provoked by OXA treatment and further provided evidence in support of concomitant activation of immunosuppressive genes by OXA. More importantly, combinational administration of OXA with the IDO1 inhibitor tremendously delayed xenograft tumor progression, which was accompanied by decreased cell proliferation and increased cell apoptosis. Meanwhile, tumor-infiltrating CD8⁺ T cells were significantly stimulated by simultaneous treatment of OXA and NLG919, and production of immunosuppressive cytokine was inhibited, and immunostimulatory cytokines were induced as well. Our data highlighted the promising therapeutic actions of a combination of OXA

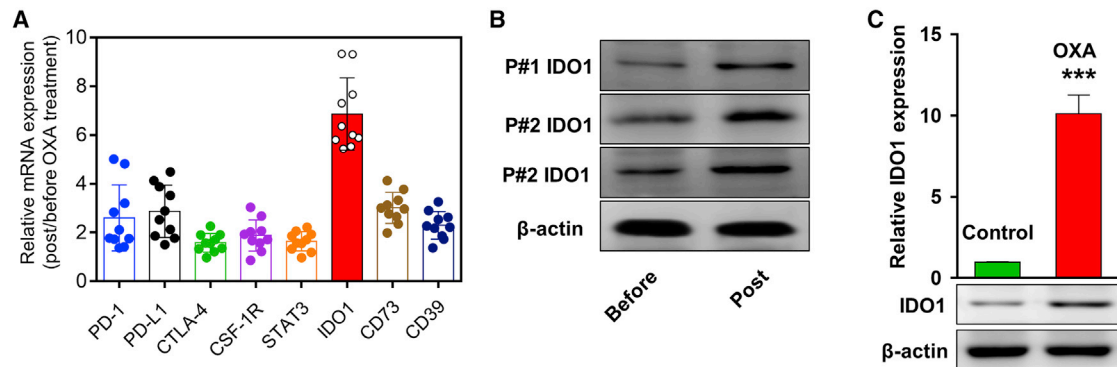


Figure 4. OXA treatment induces upregulation of IDO1 in patient-derived colorectal cancer cells

(A) Gene expression in patient-derived colorectal cancer cells post-OXA treatment. Ten colorectal cancer samples obtained from patients underwent an enzymatic digestion, and digested single cells were cultured in complete DMEM medium containing 50 μ M OXA. 2 days later, cells were harvested for the examination of gene expression. The mRNA expressions of genes associated with immunosuppression (including *PD-1*, *PD-L1*, *CTLA-4*, *STAT3*, *CD39*, *CD73*, *IDO1*, and *CSF-1R*) were examined by real-time PCR. *GAPDH* was detected as a control. (B) The protein level of IDO1 in three patient-derived colorectal cancer cells post-OXA treatment was examined by western blot. β -actin was used as a loading control. (C) IDO1 expression in the CT26 cell after OXA treatment. Data represent mean \pm SD. *** p < 0.001.

with the IDO1 inhibitor in the mouse model, which warranted further preclinical and clinical investigations.

Of note, OXA plays multiple roles in the microenvironment. As an inducer of immunogenic cell death, OXA can promote the exposure of CRT on the surface of dying tumor cells, which provides a signal to attract antigen-presenting cells, such as DCs.⁹ Furthermore, ATP and HMGB1, released by dying tumor cells, provide adjuvant stimuli for the activation of DCs.¹⁰ In this way, OXA increases cancer immunogenicity and boosts the anti-tumor immune response. On the other hand, we found that OXA could also induce IDO1 overexpression, which weakened the anti-tumor function of CD8⁺ T cells. We speculate that OXA-induced IDO1 overexpression compromises the effect of immunogenic cell death. Taking all of the above effects into consideration, we believe the overall effect of OXA treatment leads to enhanced anti-tumor immune response. In this study, we indeed confirmed that inhibitor-mediated suppression of IDO1 can synergize with OXA for cancer immunotherapy.

IDO1 was identified as a heme enzyme that catalyzes the first and rate-limiting step in tryptophan metabolism to N-formyl-kynurenine.¹⁵ Recognized pathophysiological roles of IDO1 include peripheral immune tolerance, homeostasis maintenance, and anti-microbial and anti-tumor defense.¹⁶ Recently, multiple studies suggest the suppressor role of IDO1 in anti-tumor immunity,^{17–19} which is constitutively expressed in most human cancers. Forced overexpression of IDO1 in immunogenic mouse tumor cells, which was accompanied with significant T lymphocyte proliferation arrest, blocked their rejection by preimmunized mice.²⁰ Here, we demonstrate that endogenous IDO1 of CRC was remarkably induced by OXA treatment through yet-unknown mechanisms, which consequently contributed to the immunosuppressive local microenvironment formation. Our observations were partially supported by the study performed by Sakurai et al.²¹, who reported that IDO1 activity was significantly higher post-

chemotherapy with weekly paclitaxel administration in breast cancer patients. Overactivation of IDO1 in this scenario therefore served as a perfect candidate target for therapeutic interventions. In support of our results in terms of combinational administration of OXA with the IDO1-specific inhibitor, assembling evidence uncovered the synergistic effects between IDO1 inhibitors and chemotherapy against a number of human malignancies. Muller et al.²² proposed that inhibition of IDO1 potentiated cancer chemotherapy. Jochems et al.²³ demonstrated that the IDO1-selective inhibitor, epacadostat, significantly enhanced DC immunogenicity and lytic capacity of tumor-infiltrating T cells. Hanihara et al.²⁴ showed the cooperative anti-tumor potency of IDO1 inhibition and temozolomide in a murine glioma animal model. Based on our data, we propose that combinational administration of OXA with NLG919 exerts anti-tumor activity via activating a local immune response, which definitely warrants further investigations either preclinically or clinically. Nevertheless, there are limitations in the current study. First, although NLG919 has been reported as a potent IDO pathway inhibitor,²⁵ no literature reported whether NLG919 could target other IDO isoforms, warranting further investigation. Second, over ten different IDO inhibitors are in clinical development or late preclinical testing, including NLG-919.²⁶ It would be interesting to compare their *in vitro* effect on CRC in future studies, especially since IDO inhibitors have not been very successful in human trials for solid tumors. Third, only one CRC cell line was used in the current study, and the results should be verified in a different cell line to rule out cell line-specific effects.

It is noteworthy that the molecular mechanisms underlying the OXA-upregulated IDO1 in CRC were still elusive. We speculate that epigenetic reprogramming and transcriptional activation might contribute to this phenomenon, which requires further experimental clarifications. In addition, we provide the preliminary evidence showing IDO1 upregulation by OXA *in vitro*, which warranted further confirmation in clinical samples undergoing chemotherapy.

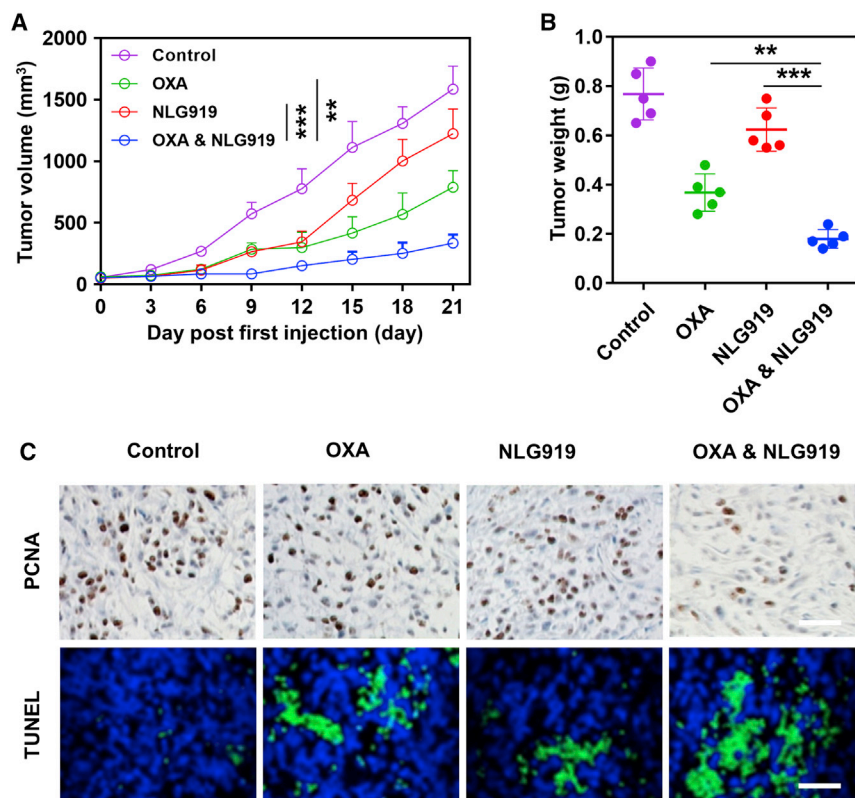


Figure 5. In vivo anti-tumor effect of OXA, NLG919, and a combination of the two agents

(A) Inhibition of tumor growth by various treatments in CT26 tumor-bearing BALB/c mice (n = 5). BALB/c mice bearing CT26 tumors of ~50 mm³ received PBS, OXA, NLG919, or a combination of OXA and NLG919 every 3 days for 5 times. The administration dosage of OXA and NLG919 was 3.0 mg/kg (intravenously [i.v.]) and 20 mg/kg (orally), respectively. Data represent mean ± SD. **p < 0.01, ***p < 0.001 (versus control group). (B) Tumor weight at the end of antitumor experiments. (C) PCNA and TUNEL data analyses of tumor tissues after treatment with various therapeutic agents. The TUNEL-positive apoptotic cells are stained green. The PCNA-positive proliferating cells are stained brown. Scale bar, 5 μm.

In summary, we hereby report the immunogenic cell death provoked by OXA in CRC, which concomitantly induces IDO1 expression and forges the local immunosuppressive microenvironment. Combinational administration of OXA and the IDO1 inhibitor manifests potent anti-tumor activity via activating the host immune response.

MATERIALS AND METHODS

Cell lines

Murine CRC cell line CT26 was obtained from the American Type Culture Collection (NY, USA) and cultured in RPMI-1640 medium

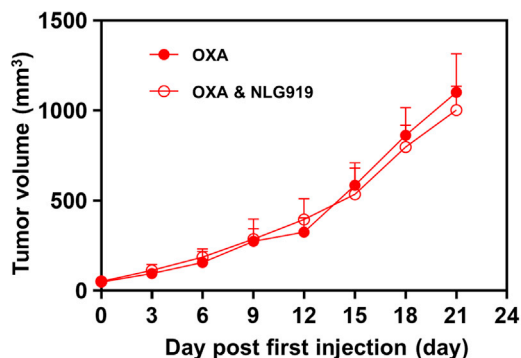


Figure 6. Inhibition of tumor growth by OXA or OXA and NLG919 in CT26 tumor-bearing BALB/c nude mice

supplemented with 5% fetal bovine serum (FBS; Invitrogen, Waltham, MA, USA) and 1% penicillin/streptavidin (Invitrogen). Mycoplasma contamination was regularly excluded with the PCR method.

Xenograft tumor mouse model

Immunodeficient BALB/c mice (T cell deficiency, BALB/c nude, 6-week-old females) and normal immune BALB/c (wild-type mice, 6-week-old females) were used to establish the murine CRC tumor model (subcutaneous injection of 10⁶ CT26 cells in the back). The animals were obtained from Shanghai Yunhao Biotech Center (Shanghai, China) and maintained in a specific-pathogen-free (SPF)-grade environment. OXA (3 mg/kg) was administrated until tumor volume approached 50 mm³, once every 3 days for four consecutive times. Xenograft tumor and survival of mice were regularly monitored. Animal-related study was approved by the Institutional Animal Care and Use Committee of Wuxi People's Hospital and in strict accordance with NIH guidelines.

Flow cytometry

CT26 cells were plated in 6-well plates and subjected to OXA treatment (50 μM) for 24 h. The indicated cells were collected by trypsin digestion and stained with both propidium iodine (PI) and phycoerythrin (PE)-conjugated anti-CRT antibody (PE-anti-CRT) on ice for 30 min. Isotype-matched immunoglobulin G (IgG) antibodies were used as control, and the fluorescent intensity of stained cells was analyzed on Gallios Flow Cytometry (Beckman Coulter, Carlsbad, CA, USA).

Immunofluorescence

Both vehicle and OXA-treated CT26 cells were plated on coverslips and allowed for attachment overnight. Cells were then fixed with 0.25% paraformaldehyde for 10 min and incubated with indicated primary antibodies at 4°C overnight. After three washes with ice-cold phosphate-buffered saline (PBS), cells were incubated with Alexa

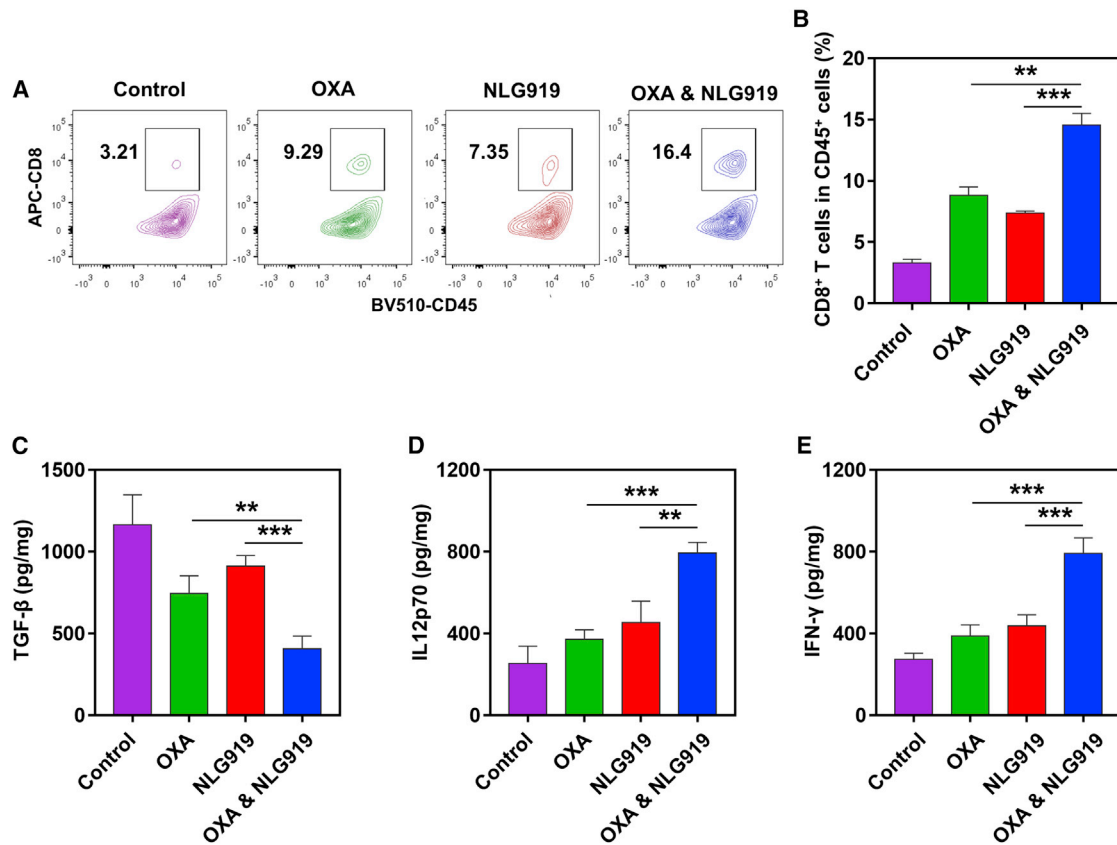


Figure 7. Flow cytometry analysis of CD8⁺ T cell subsets and ELISA analysis of cytokine expression in tumor tissues

(A) Flow cytometry gating and (B) histogram analysis of cytotoxic T cells (CD8⁺ T cells) in the CD45⁺ tumor-infiltrating lymphocyte in tumor tissues from mice receiving indicated treatment. Data represent mean \pm SD. ** $p < 0.01$, *** $p < 0.001$. (C–E) ELISA results of cytokine production in the tumors from mice receiving indicated treatments: (C) TGF- β , (D) IL12p70, and (E) IFN- γ . Data represent mean \pm SD. * $p < 0.05$, ** $p < 0.01$, *** $p < 0.001$.

594-conjugated secondary antibody for 30 min at room temperature. Nuclei were counterstained with 4',6-diamidino-2-phenylindole (DAPI) for another 30 min and followed by mounting with ProLong Gold Antifade Mountant (Thermo Fisher Scientific, Waltham, MA, USA). The representative images were captured with a Leica Confocal System (Hilden, Germany).

Detection of HMGB1 release

CT26 cells were plated in 6-well plates and followed by OXA treatment for 24 h. Cell culture supernatants were collected at indicated time points, cell debris was removed by centrifugation, and secreted HMGB1 was measured using a Human HMGB1/HMG-1 ELISA Kit (Novus Biologicals, Littleton, CO, USA), following the manufacturer's instructions.

ATP measurement

Secretory ATP content was measured with an ATP Determination Kit (Thermo Fisher Scientific, Carthage, MO, USA), according to the manufacturer's recommendations. The conditioned media were collected, and all cell debris was completely removed by centrifuga-

tion. An equal volume of cell culture supernatant and ATP reaction mix was incubated at room temperature for 30 min, and absorption at 570 nm was measured with a Multimode Microplate Reader (Bertold, Oak Ridge, TN, USA).

Real-time PCR

PCR reaction was performed on an ABI Prism 7900 PCR Detection System (Thermo Fisher Scientific, Carthage, MO, USA). Relative expression of target genes was normalized to glyceraldehyde 3-phosphate dehydrogenase (GAPDH) and calculated using the $2^{-\Delta\Delta Ct}$ method. Total RNA was extracted with TRIzol reagent (Invitrogen) and reversely transcribed with a High Capacity cDNA Synthesis Kit (Tiangen, Beijing, China). SYBR Green was used to measure product DNA. All primer sequences were listed as below:

PD-1 forward (F): 5'-CCAGGATGGTTCTTAGACTCCC-3'

PD-1 reverse (R): 5'-TTTAGCAGGAAGCTCTCCGAT-3'

PD-L1 F: 5'-TGGCATTGTCTGAACGCATTT-3'

PD-L1 R: 5'-TGCAGCCAGGTCTAATTGTTTT-3'

CTLA-4 F: 5'-GCCCTGCACTCTCCTGTTTTT-3'
 CTLA-4 R: 5'-GGTTGCCGCACAGACTTCA-3'
 CSF-1R F: 5'-GGGAATCCCAGTGATAGAGCC-3'
 CSF-1R R: 5'-TTGGAAGGTAGCGTTGTTGGT-3'
 STAT3 F: 5'-CAGCAGCTTGACACACGGTA-3'
 STAT3 R: 5'-AAACACCAAAGTGGCATGTGA-3'
 IDO1 F: 5'-GCCAGCTTCGAGAAAGAGTTG-3'
 IDO1 R: 5'-ATCCCAGAACTAGACGTGCAA-3'
 CD73 F: 5'-GCCTGGGAGCTTACGATTTTG-3'
 CD73 R: 5'-TAGTGCCCTGGTACTGGTCG-3'
 CD39 F: 5'-AGGTGCCTATGGCTGGATTAC-3'
 CD39 R: 5'-CCAAAGCTCCAAAGGTTTCCT-3'

Western blot

Cells were washed with sterile ice-cold PBS and lysed in strong radioimmunoprecipitation buffer for 30 min. Proteins were resolved by 12% sodium dodecyl sulfate-polyacrylamide gel electrophoresis and transferred onto polyvinylidene fluoride membranes (Millipore, St. Louis, MO, USA). Blots were detected with indicated primary antibodies (rabbit anti-CRT, 1:5,000, ab2907, and rabbit anti- β -actin, 1:2,000, ab8227, from Abcam, Shanghai, China; mouse anti-BSA, 1:1,000, B2901, and rabbit anti-IDO1, 1:1,000, HPA023149, from Sigma, St. Louis, MO, USA) at 4°C overnight, followed by incubation with horseradish peroxidase (HRP)-labeled secondary antibody (goat anti-rabbit, #7074, 1:5,000, and horse anti-mouse, #7076, 1:5,000, from Cell Signaling Technology, Danvers, MA, USA), and visualized with an enhanced chemiluminescence kit (Millipore, Billerica, MA, USA).

Generation of BMDCs

Bone marrow cells were collected in RPMI-1640 media from tibias and femurs of BALB/c mice. Red blood cells were lysed in Tris-ammonium chloride for 2 min, and bone marrow cells were seeded in 6-well plates precoated with recombinant mouse FLT3 ligand (R&D Systems, Minneapolis, MN, USA). The suspension cells were collected for co-culture with tumor cells.

IHC

Rabbit anti-PCNA antibody (Sigma) was incubated with tissue sections at 4°C overnight, followed by incubation with biotin-labeled goat anti-rabbit secondary antibody at room temperature for 1 h. After hybridization with streptavidin-HRP, diaminobenzidine (DAB) was applied for a chromogenic reaction. Sections were counterstained with hematoxylin.

TUNEL staining

The *In situ* Apoptosis Detection Kit and peroxidase (POD; Roche, Basel, Switzerland) were used for TUNEL labeling following the manufacturer's manual. Tissue slides were briefly digested with Proteinase

K and incubated with TdT reaction mix at 37°C for 1 h, which was followed by a converter-POD for 30 min. The apoptotic index was estimated as the percentage of TUNEL-positive cells.

Statistical analyses

All results were presented as mean \pm SD unless specified in figure legends. Statistical analyses were conducted using Student's t test and one or two-way ANOVA analysis, followed by a post hoc test with SPSS 23.0 software (San Diego, CA, USA). Experiments were repeated at least three times. p values were two tailed, and p < 0.05 was considered a significant difference.

ACKNOWLEDGMENTS

The study was supported by the National Natural Science Foundation of China (81371683 and 81702592); Wuxi Medical Emphasis Disciplines Funding (syxzdxx-pwk); Wuxi Science and Technology Development Plan (CZE02H1701); Clinical Medicine Project of Jiangsu Province (BL2014023); and National Sciences Foundation of Jiangsu Province (BK20160198).

AUTHOR CONTRIBUTIONS

X.M. and T.W. conceived and designed the study and wrote the manuscript. X.M., Y.Z., Z.L., L.H., T.X., R.S., and T.W. collected and assembled the data. X.M., Y.Z., and Z.L. performed the statistical analysis. All authors read and approved the final manuscript.

DECLARATION OF INTERESTS

The authors declare no competing interests.

REFERENCES

- Mármol, I., Sánchez-de-Diego, C., Pradilla Dieste, A., Cerrada, E., and Rodríguez Yoldi, M.J. (2017). Colorectal Carcinoma: A General Overview and Future Perspectives in Colorectal Cancer. *Int. J. Mol. Sci.* 18, 197.
- Siegel, R.L., Miller, K.D., and Jemal, A. (2019). Cancer statistics, 2019. *CA Cancer J. Clin.* 69, 7–34.
- Cho, Y.A., Lee, J., Oh, J.H., Chang, H.J., Sohn, D.K., Shin, A., and Kim, J. (2019). Genetic Risk Score, Combined Lifestyle Factors and Risk of Colorectal Cancer. *Cancer Res. Treat.* 51, 1033–1040.
- Ciombor, K.K., Wu, C., and Goldberg, R.M. (2015). Recent therapeutic advances in the treatment of colorectal cancer. *Annu. Rev. Med.* 66, 83–95.
- Huang, Y., Li, L., Liu, W., Tang, T., and Chen, L. (2020). The progress of CAR-T therapy in cancer and beyond. *STEMedicine* 1, e47.
- Ciardello, D., Vitiello, P.P., Cardone, C., Martini, G., Troiani, T., Martinelli, E., and Ciardiello, F. (2019). Immunotherapy of colorectal cancer: Challenges for therapeutic efficacy. *Cancer Treat. Rev.* 76, 22–32.
- Binnewies, M., Roberts, E.W., Kersten, K., Chan, V., Fearon, D.F., Merad, M., Coussens, L.M., Gabrilovich, D.L., Ostrand-Rosenberg, S., Hedrick, C.C., et al. (2018). Understanding the tumor immune microenvironment (TIME) for effective therapy. *Nat. Med.* 24, 541–550.
- Baratelli, C., Zichi, C., Di Maio, M., Brizzi, M.P., Sonetto, C., Scagliotti, G.V., and Tampellini, M. (2018). A systematic review of the safety profile of the different combinations of fluoropyrimidines and oxaliplatin in the treatment of colorectal cancer patients. *Crit. Rev. Oncol. Hematol.* 122, 21–29.
- Sun, F., Cui, L., Li, T., Chen, S., Song, J., and Li, D. (2019). Oxaliplatin induces immunogenic cells death and enhances therapeutic efficacy of checkpoint inhibitor in a model of murine lung carcinoma. *J. Recept. Signal Transduct. Res.* 39, 208–214.

10. Zhou, J., Wang, G., Chen, Y., Wang, H., Hua, Y., and Cai, Z. (2019). Immunogenic cell death in cancer therapy: Present and emerging inducers. *J. Cell. Mol. Med.* *23*, 4854–4865.
11. Casares, N., Pequignot, M.O., Tesniere, A., Ghiringhelli, F., Roux, S., Chaput, N., Schmitt, E., Hamai, A., Hervas-Stubbs, S., Obeid, M., et al. (2005). Caspase-dependent immunogenicity of doxorubicin-induced tumor cell death. *J. Exp. Med.* *202*, 1691–1701.
12. Cui, S. (2017). Immunogenic Chemotherapy Sensitizes Renal Cancer to Immune Checkpoint Blockade Therapy in Preclinical Models. *Med. Sci. Monit.* *23*, 3360–3366.
13. Bains, S.J., Abrahamsson, H., Flatmark, K., Dueland, S., Hole, K.H., Seierstad, T., Redalen, K.R., Meltzer, S., and Ree, A.H. (2020). Immunogenic cell death by neoadjuvant oxaliplatin and radiation protects against metastatic failure in high-risk rectal cancer. *Cancer Immunol. Immunother.* *69*, 355–364.
14. Jessup, J.M., Kabbout, M., Korokhov, N., Joun, A., Tollefson, A.E., Wold, W.S.M., and Mattoo, A.R. (2020). Adenovirus and Oxaliplatin cooperate as agnostic sensitizers for immunogenic cell death in colorectal carcinoma. *Hum. Vaccin. Immunother.* *16*, 636–644.
15. Zitron, I.M., Kamson, D.O., Kiousis, S., Juhász, C., and Mittal, S. (2013). In vivo metabolism of tryptophan in meningiomas is mediated by indoleamine 2,3-dioxygenase 1. *Cancer Biol. Ther.* *14*, 333–339.
16. Liu, M., Wang, X., Wang, L., Ma, X., Gong, Z., Zhang, S., and Li, Y. (2018). Targeting the IDO1 pathway in cancer: from bench to bedside. *J. Hematol. Oncol.* *11*, 100.
17. Munn, D.H., and Mellor, A.L. (2013). Indoleamine 2,3 dioxygenase and metabolic control of immune responses. *Trends Immunol.* *34*, 137–143.
18. Schmidt, S.V., and Schultze, J.L. (2014). New Insights into IDO Biology in Bacterial and Viral Infections. *Front. Immunol.* *5*, 384.
19. Uyttenhove, C., Pilotte, L., Théate, I., Stroobant, V., Colau, D., Parmentier, N., Boon, T., and Van den Eynde, B.J. (2003). Evidence for a tumoral immune resistance mechanism based on tryptophan degradation by indoleamine 2,3-dioxygenase. *Nat. Med.* *9*, 1269–1274.
20. Qian, F., Vilella, J., Wallace, P.K., Mhawech-Fauceglia, P., Tario, J.D., Jr., Andrews, C., Matsuzaki, J., Valmori, D., Ayyoub, M., Frederick, P.J., et al. (2009). Efficacy of levo-1-methyl tryptophan and dextro-1-methyl tryptophan in reversing indoleamine-2,3-dioxygenase-mediated arrest of T-cell proliferation in human epithelial ovarian cancer. *Cancer Res.* *69*, 5498–5504.
21. Sakurai, K., Enomoto, K., Kitajima, A., Tani, M., Amano, S., and Shiono, M. (2008). [Indoleamine 2,3-dioxygenase expression in breast cancer patients during chemotherapy]. *Gan To Kagaku Ryoho* *35*, 2265–2267.
22. Muller, A.J., DuHadaway, J.B., Donover, P.S., Sutanto-Ward, E., and Prendergast, G.C. (2005). Inhibition of indoleamine 2,3-dioxygenase, an immunoregulatory target of the cancer suppression gene Bin1, potentiates cancer chemotherapy. *Nat. Med.* *11*, 312–319.
23. Jochems, C., Fantini, M., Fernando, R.I., Kwilas, A.R., Donahue, R.N., Lepone, L.M., Grenga, I., Kim, Y.S., Brechbiel, M.W., Gulley, J.L., et al. (2016). The IDO1 selective inhibitor epacadostat enhances dendritic cell immunogenicity and lytic ability of tumor antigen-specific T cells. *Oncotarget* *7*, 37762–37772.
24. Hanihara, M., Kawataki, T., Oh-Oka, K., Mitsuka, K., Nakao, A., and Kinouchi, H. (2016). Synergistic antitumor effect with indoleamine 2,3-dioxygenase inhibition and temozolomide in a murine glioma model. *J. Neurosurg.* *124*, 1594–1601.
25. Mautino, M.R., Jaipuri, F.A., Waldo, J., Kumar, S., Adams, J., Van Allen, C., Marciniowicz-Flick, A., Munn, D., Vahanian, N., and Link, C.J. (2013). Abstract 491: NLG919, a novel indoleamine-2,3-dioxygenase (IDO)-pathway inhibitor drug candidate for cancer therapy. In Proceedings of the 104th Annual Meeting of the American Association for Cancer Research, *73*, p. 491.
26. Labadie, B.W., Bao, R., and Luke, J.J. (2019). Reimagining IDO Pathway Inhibition in Cancer Immunotherapy via Downstream Focus on the Tryptophan-Kynurenine-Aryl Hydrocarbon Axis. *Clin. Cancer Res.* *25*, 1462–1471.